LORENTZ-FORCE INDEPENDENCE OF DIFFERENTIAL CURRENT-VOLTAGE CHARACTERISTIC IN HTSC CERAMICS

O. V. Geraschenko, S. L. Ginzburg, I. D. Luzyanin, A. I. Sibilev, M. A. Pustovoit, V. P. Khavronin

It is a common practice that both flux penetration and energy dissipation in type-II superconductors are determined by supercritical or thermally activated vortices motion due to the Lorentz force. The Lorentz-force dependence can be checked either measuring the integral current-voltage characteristics (CVC) as a function of the angle between the current and applied magnetic field directions or measuring the quantities characterizing the ac low field penetration into the superconductor as a function of the angle between the ac low and dc strong fields.

In the present work, we have demonstrated that both the integral CVC and the ac low field penetration into the ceramic high-T_c superconductors are Lorentz-force independent, i.e. ones are not related with a vortices motion. This contradicts to current ideas.

The measurements of the CVC and the study of the ac low field penetration were carried out on few usual ceramic samples of $YBa_2Cu_3O_{7-x}$ prepared by the standard technology.

The four-terminal CVC measurements were done on the thin slabs. The sample was equipped with two current and four voltage leads. Thus, there was a possibility to measure the voltage both along and across the current directed along the z-axis. The *dc* magnetic field directed in the yz-plane formed the angle α with respect to the current direction (see insertion to Fig.1a). After sample cooling at $H = 0$, the external magnetic field was applied and the current was switched on. Fig.1a shows the results of such measurements for $T \approx 78$ K. From this figure, one can see that all CVC fully coincide with each other and the voltage across the current equals zero. The CVC coincidence for the angles 0° and $\pi/2$ was observed in the range 78–90 K (Fig.1b). The measurements of the specific resistance ρ were also performed at $\alpha = 0°$ and $\pi/2$. In this case the dependencies $\rho(T)$ were also coincided. Thus, the CVC

do not depend on the angle a between the current and the magnetic field neither in the supercritical nor thermally activated regions.

The studies of the ac field penetration were carried out on samples shaped in the form of a disc. Two mutually perpendicular coils were wound on the sample. The coil axes were directed along axis z and y, respectively. In the experiments the projections $C_{kz,y}$ of the higher harmonics of response $b(t)$ on the field $\vec{H}(t) = H\vec{e}_z + h_0\vec{n}_0 \cos\omega t$ have been measured. Here H and h_0 are the amplitudes of dc and ac fields, respectively, γ is the angle between the vectors $\vec{e}_{xy}$ and $\vec{n}_0$, $\vec{n}_0 = \vec{e}_z \cos\gamma + \vec{e}_y \sin\gamma$.

The results of these studies have shown that the odd harmonics $C_{3z} \sim \cos\gamma$ and $C_{3y} \sim \sin\gamma$ (Figs.2a and 2b). The even harmonics $C_{2z} \sim \cos^2\gamma$ and $C_{2y} \sim \cos\gamma \sin\gamma$ (Figs.3a and 3b). Such behavior of higher harmonics was observed practically up to T_c at $h_0 \ll H \approx 1 - 5\ Oe$.

Note, that there are three alternative theories describing the magnetic field penetration due to the manipulation changing the direction of external field: (I) the usual critical state theory related to pinning, (II) the concept of flux-line-cutting (FLC) also taking into consideration the pinning and (III) the phenomenological theory proposed by Bean. These theories are different by the differential CVC. The concept of flux-linecutting corresponds to the FLC-CVC. The usual equation of critical state is the particular case of the FLC. We shall describe the Bean theory by the isotropic spatial CVC (ISCVC).

Let us consider a superconductor of thickness d along x-axis and infinite in the y- and z-directions. The external field H is directed along the z-axis in the yz-plane. It is obvious that in such geometry $\vec{B}$, $\vec{E}$ and $\vec{j}$ are vectors in yz-plane and depend on x only. In this case Maxwell equations, the FLC-CVC (II) and the ISCVC (III) are given by

$$\frac{\partial \vec{B}}{\partial t} = -\vec{e}_x \times \frac{\partial \vec{E}}{\partial x}, \quad 4\pi\vec{j} = \vec{e}_x \times \frac{\partial \vec{B}}{\partial x}, \quad \mu = 1,$$

$$\vec{j} = j_{cII}\frac{\vec{B}}{B}\mathrm{sign}E_{II} + j_{cI}\frac{\vec{B}\times\vec{e}_x}{B}\mathrm{sign}E_{\perp}, \qquad (II)$$

$$E_{II} = \frac{\vec{E}\vec{B}}{B}, \quad E_{\perp} = \frac{\vec{E}(\vec{B}\times\vec{e}_x)}{B},$$

$$\vec{j} = j_c\frac{\vec{E}}{E} \qquad (III). \qquad (1)$$

Here j_{cII} and j_{cI} are current densities parallel and perpendicular to $\vec{B}$, respectively. The model (I) becomes (II) at $j_{cII} = \infty$, in this case the term containing j_{cII} disappears.

The comparison of FLC-CVC and ISCVC models shows that they are principally different: the FLC-CVC depends strongly on the angle between $\vec{B}$ and $\vec{j}$, i.e. on the Lorentz force, while the ISCVC does not depend on this angle i.e. the Lorentz-force independence. It is naturally expected that the expressions describing the response to an ac field are different for the both models and, as a consequence, these models can be distinguished experimentally.

For the FLC model the expression of the higher harmonics of induction can be represented (in the case of $h_{Oz,y} \ll H$) by:

$$C_{3z} = \frac{h_0^2\cos^2\gamma}{15\pi^2 j_{c\perp}(H)d}, \quad C_{3y} = \frac{h_0^2\sin^2\gamma}{15\pi^2 j_{cII}(H)d},$$

$$C_{2z} = \frac{h_0^3\cos^3\gamma}{15\pi^2 d}\frac{d}{dH}\left\{\frac{1}{j_{c\perp}(H)}\right\}, \quad C_{2y} = 0 \qquad (2)$$

The expressions for induction harmonics are others for the model (III):

$$C_{3z} = \frac{h_0^2 \cos^2\gamma}{15\pi^2 j_c(H) d}, \quad C_{3y} = \frac{h_0^2 \sin^2\gamma}{15\pi^2 j_c(H) d},$$
$$C_{2z} = \frac{h_0^3 \cos^3\gamma}{15\pi^2 d} \frac{d}{dH}\left\{\frac{1}{j_c(H)}\right\}, \quad C_{2y} = \frac{h_0^3 \cos\gamma \sin\gamma}{15\pi^2 d} \frac{d}{dH}\left\{\frac{1}{j_c(H)}\right\} \qquad (3)$$

Thus, the comparison of the obtained experimental data with (1)–(3) has turned out be in a favour of the ISCVC model. Actually, the CVC measured do not depend on the angle between the current and the magnetic field and the odd harmonics are proportional to $\cos\gamma$ (or $\sin\gamma$) but not $\cos^2\gamma$ (or $\sin^2\gamma$) in the contradiction to the FLC model. Besides, in our experiments the second harmonic C_{2y} was observed at all values of $h_{Oz,y}$ (except $h_{0z} = 0$).

The physical picture of the Lorentz-force independence appears to us as follows. Notice that the ceramic HTSC is the Josephson medium which is characterized by two parameters — the Josephson current density j_c and the grain size a. If the condition $j_c a^3 \ll \Phi_0$ (Φ_0 is the fiux quantum) holds, the Josephson medium can be considered in the continuum limit because the depth length $\lambda \sim a(\Phi_0/j_c a^3)^{1/2} \gg a$ in this medium. In this case a picture of usual type-II superconductor arises in which of the CVC is determined by the Lorentz force $\vec{F} \sim \vec{j} \times \vec{H}$ and the pinning. However, if the alternative condition $j_c a^3 \gg \Phi_0$ holds, $\lambda \ll a$ and the concept of vortex disappear. It can be shown that in this case the Josephson medium is transformed into the system in which the pinning takes place on the element Josephson contacts. Here the nonlinear properties of these contacts are "worked". If the current $j < j_c$, this contact turns into in the superconducting state and there is the pinning. If $j > j_c$, this contact turns into in the normal state and the flux quantum penetrates through it. Then the condition $j > j_c$ is important and the vector product $\vec{j} \times \vec{H}$ does not arise. It is clear that this physical picture results in the isotropic spatial CVC (ISCVC) without fail.

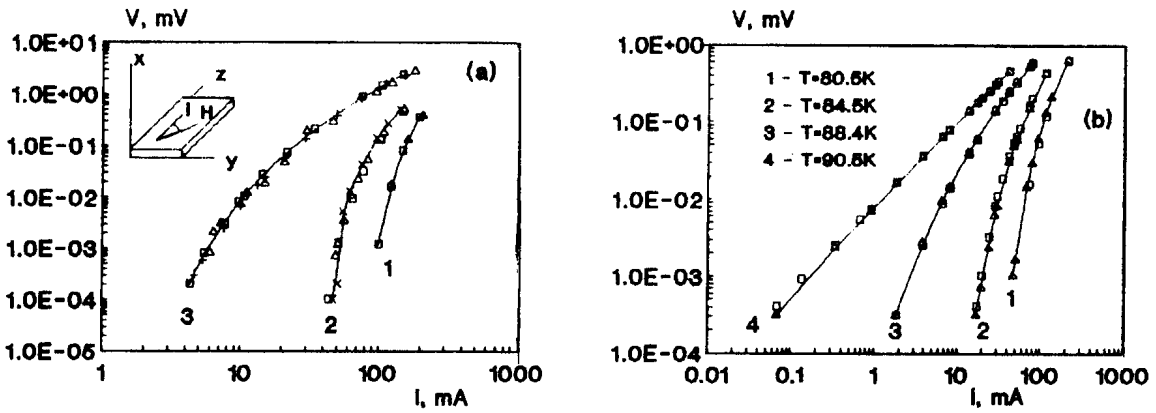

Fig.1. (a). The CVC at $H = 1.2\ Oe$ (1), $H = 3.0\ Oe$ (2), $H = 9.4\ Oe$ (3) and at the various angles α (0° — Δ, 45° — +, 63° — x, 90° — □);
(b). The CVC at $H = 9.3\ Oe$, $\alpha = 0°$ (Δ), $\alpha = \pi/2$ (□) and at the various temperatures

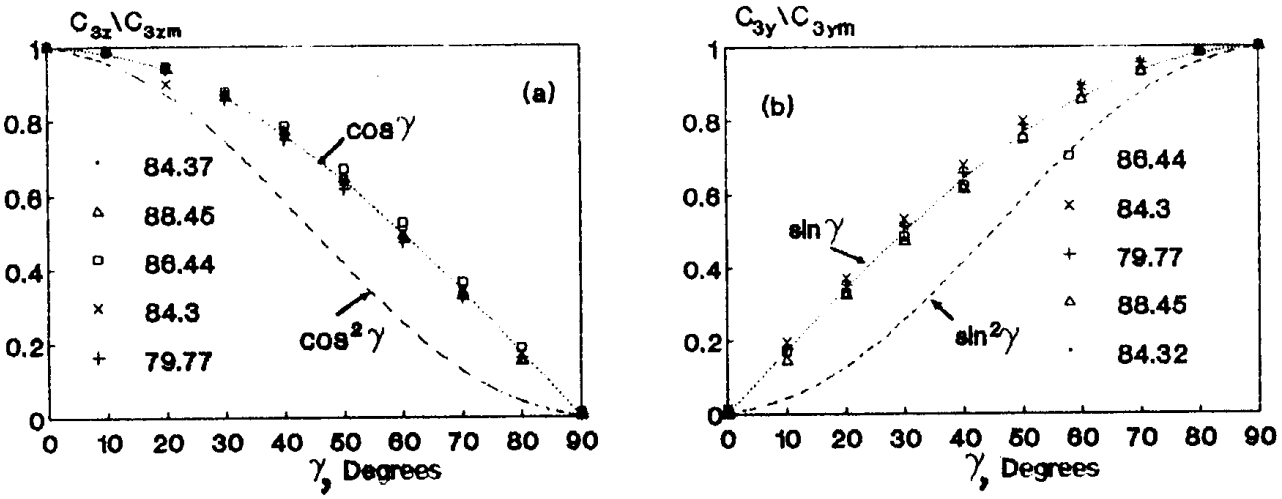

Fig.2. (a,b). The angle dependencies of values of third harmonic reduced to $C_{3z,y}$ values measured at $\gamma = 0$, $H = 3\ Oe$ and at the various temperatures $T(K)$. For comparison the $C_{3z,y}$ vs γ (at $H = 0$) and the theoretical curves corresponding to $\cos\gamma, \cos^2\gamma$ and $\sin\gamma$, $\sin^2\gamma$ are shown

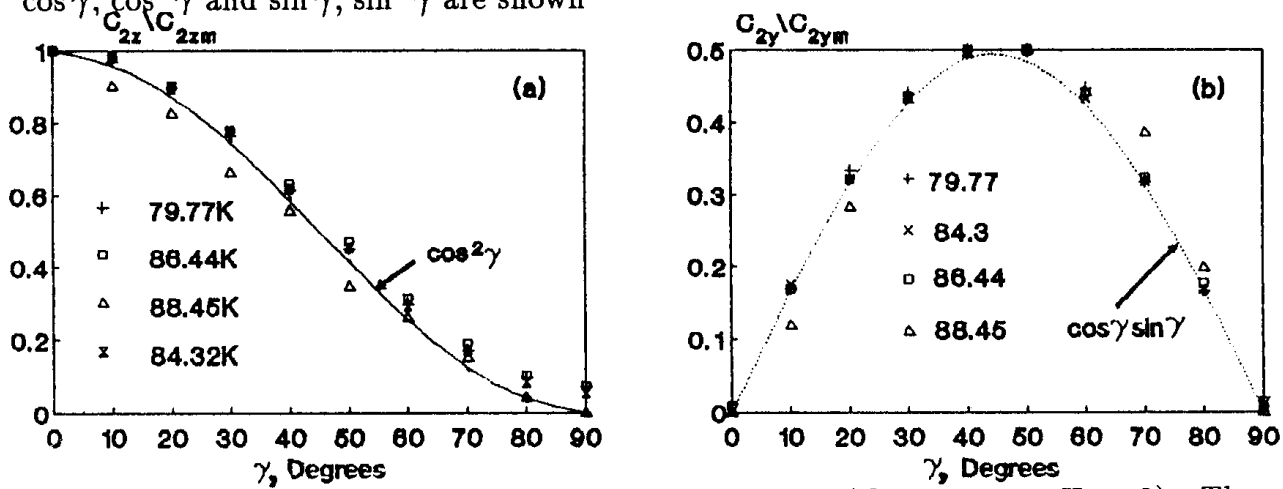

Fig.3. (a,b). The same but for the second harmonic. ($C_{2z,y} = 0$ at $H = 0$). The corresponding theoretical curves are shown also